

PACS numbers: 78.20.Ci, 78.67.Sc, 81.05.Qk, 81.07.Pr, 81.40.Tv, 82.35.Np, 85.60.-q

Morphological and Optical Properties of Polyvinyl Alcohol– Tungsten Carbide Nanostructures for Optoelectronic Nanodevices

Majeed Ali Habeeb and Zanab Ibrahim Zike

*College of Education for Pure Sciences,
Department of Physics,
University of Babylon,
Hillah, Iraq*

The PVA/WC nanocomposites are formed by using a solution casting method with varying weight percentages of WC nanoparticles: 0, 1, 2, and 3 wt.%. The optical properties of films are studied by means of the optical microscope. As revealed with optical microscope, the tungsten carbide nanoparticles form a continuous network inside the polymer (polyvinyl alcohol); the nanoparticles linked in this network include routes for charge carriers to transport through the nanocomposite, causing a shift in the material properties. The findings expose that, as the concentration of WC nanoparticles rises, the absorption coefficient, extinction coefficient, refractive index, real and imaginary dielectric constants, optical conductivity are increasing. The transmittance drops as the concentration of WC nanoparticles increases. The optical energy gap for PVA is reduced from 4.4 eV for pure PVA to 3.8 eV and is reduced from 3.7 eV to 3.1 eV for allowed and forbidden indirect transition, respectively, when the WC-nanoparticles' concentration reached 3 wt.%. This behaviour makes it suitable for a variety of optical applications.

Нанокompозити полівінілового спирту (ПВС) з наночастинками карбиду Вольфраму ПВС/WC формуються методом лиття в розчин з різним ваговим відсотком наночастинок WC: 0, 1, 2 і 3 мас.%. Оптичні властивості плівок вивчаються за допомогою оптичного мікроскопа. Як виявилось за допомогою оптичного мікроскопа, наночастинки карбиду Вольфраму утворюють безперервну мережу всередині полімеру ПВС; наночастинки, пов'язані в цій мережі, включають маршрути для транспорту носіїв заряду через нанокompозит, викликаючи зміну властивостей матеріалу. Одержані дані показують, що зі зростанням концентрації наночастинок WC зростають коефіцієнт поглинання, коефіцієнт згасання, показник заломлення, дійсна й уявна діелектричні проникності, оптична провідність. Коефіцієнт пропускання падає зі збільшенням

концентрації наночастинок WC. Оптична енергетична щільність для ПВС зменшується з 4,4 еВ для чистого ПВС до 3,8 еВ і зменшується з 3,7 еВ до 3,1 еВ для дозволеного та забороненого непрямого переходу відповідно, коли концентрація WC-наночастинок досягає 3 мас.%. Така поведінка робить його придатним для різноманітних оптичних застосувань.

Key words: nanocomposites, tungsten carbide nanoparticles, optical characteristics.

Ключові слова: наноккомпозити, наночастинки карбиду Вольфраму, оптичні характеристики.

(Received 8 April, 2023)

1. INTRODUCTION

Nanotechnology has created a different part of study for the dispensation and creation of nanomaterials, which are substances that typically have crystallite sizes of less than 100 nanometres [1, 2]. Nanotechnology is a hot theme this time, reaching, since new changes in technique physics, to precisely new fields to educating novel materials with nanometer dimensions scale. That is fast emerging and rising, with vast fields in various research approaches, advancement, and industrialized activities. Nanoparticles with higher thermal conductivity than their surrounding liquid have been found to improve deferral effective thermal conductivity [3, 4].

Polymer matrix nanocomposites are an appealing and important part of today's materials because of their low weight, simple manufacturability, low cost, high fatigue strength, and good corrosion resistance. The addition for nanoparticles into a polymer matrix meaningfully alters its physical material properties such as (structural–electrical–thermal–optical properties) [5, 6]. The polyvinyl alcohol (PVA) is good host medium for extensive variety for nanoparticles. It is motivated by the view of producing ultratransparent films with superior optical properties. They have received a lot of attention due to their excellent dielectric properties. Their flexibility is exceptional, and their dielectric strength is quite robust. The metal or alloy doped into ceramic of dielectric materials has received a lot of attention over the last few years. While exist (as chemically–thermally stable) even at high temperatures, the WC transition-metal carbide ceramic exhibits outstanding high-temperature strength and good erosion resistance. The electrical and optical characteristics are typically metallic [7, 8]. This paper aims to preparation and properties of polyvinyl alcohol/tungsten carbide nanocomposites (NCs) for employed in different optoelectronic applications.

2. EXPERIMENTAL PART

The PVA/WC nanocomposites films were made using the casting method at different weight percentages, 0, 1, 2, and 3 wt.%, by dissolved 1 g of polyvinyl alcohol in 40 ml of distilled water at temperature 70°C for 30 minutes with magnetic stirrer and added tungsten carbide nanoparticles (NPs). PVA/WC nanocomposites are tested in different concentrations using an Olympus type Nikon-73346 optical microscope that has a magnifying power of $\times 10$ and equipped with a camera used in the microscopic photography. The optical properties for PVA/WC nanocomposites' films were measured by a double beam spectrophotometer (UV-1800 from Shimadzu) at wavelength between 220 and 820 nm.

The formula shown below is used to calculate absorbance [9, 10]:

$$A = I_A/I_O; \quad (1)$$

I_A is the intensity of light that is absorbed by the substance; I_O is the intensity of light that is incident.

The formula below can be used to calculate transmittance T [11]:

$$T = I_T/I_O; \quad (2)$$

I_T is the intensity of light transmitted through a material; I_O is the intensity of light that is incident.

We can measure the absorption coefficient α of the current materials by use the thickness of the film [12, 13]:

$$\alpha = 2.303A/d; \quad (3)$$

here, A represents absorbance; film thickness is represented by d .

The indirect transition was formed by applying the relation [14, 15]:

$$\alpha h\nu = B(h\nu - E_g)^r; \quad (4)$$

$r=2$ for permitted indirectly transitions and $r=3$ for proscribed indirectly transitions; $h\nu$ the incident photon energy; B is constant value, and E_g is optical band gap.

The refractive index n can be determined as follows [16, 17]:

$$n = \sqrt{\frac{4R - k^2}{(R - 1)^2} - \frac{(R + 1)}{(R - 1)}}; \quad (5)$$

R is reflectance. The equation shown below can be used to determine

the extinction coefficient k [18, 19]:

$$k = \alpha\lambda/(4\pi). \quad (6)$$

The wavelength of the incident light is indicated here by λ .

The real (ϵ_1) and imaginary (ϵ_2) components of the dielectric constant are determined by the following formulae [20, 21]:

$$\epsilon_1 = n^2 - k^2, \quad (7)$$

$$\epsilon_2 = 2nk. \quad (8)$$

The optical conductivity σ is calculated from the equation [22]

$$\sigma = \alpha nc/(4\pi), \quad (9)$$

where light velocity is denoted by c .

3. RESULTS AND DISCUSSION

Images of optical microscope for (PVA/WC) nanocomposites films taken at a magnification power of $\times 10$ for all samples at various concentrations are shown in Fig. 1. We can see $a-d$, once the concentration for tungsten carbide nanoparticles reaches 3 wt.%, the nanoparticles form a continuous network inside the polymer. The nanoparticles linked in this network include routes for charge carriers to transport through NCs, causing a shift in the material properties [23, 24].

The relation between absorbance and wavelength for PVA/WC nanocomposites is displayed in Fig. 2. The figure demonstrates that, as the wavelength increases, the absorbance of films decreases, peaking close to the fundamental absorption edge 220 nm. In general, visible and near-infrared absorbances of film are minimal. We can explain this performance in this way. Near the fundamental

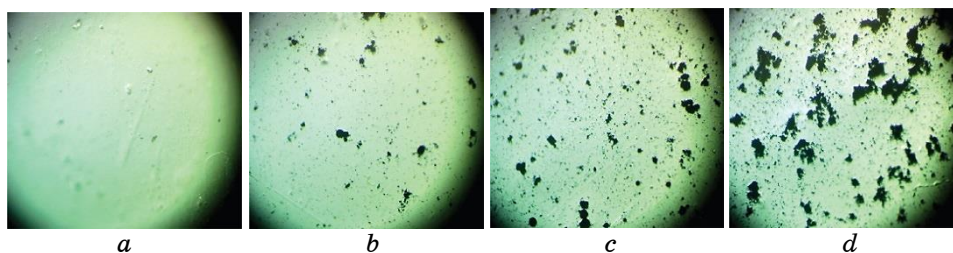


Fig. 1. The photomicrographs of PVA/WC nanocomposites: (a) for (PVA); (b) for 1 wt.% WC NPs; (c) for 2 wt.% WC NPs; (d) for 3 wt.% WC NPs.

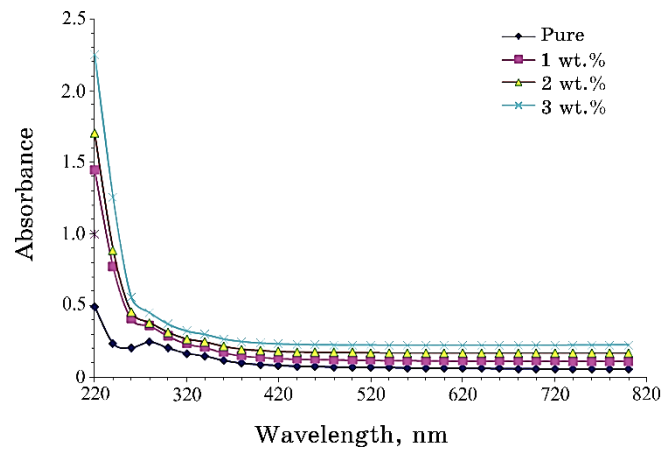


Fig. 2. The relation between absorbance and wavelength for PVA/WC nanocomposites.

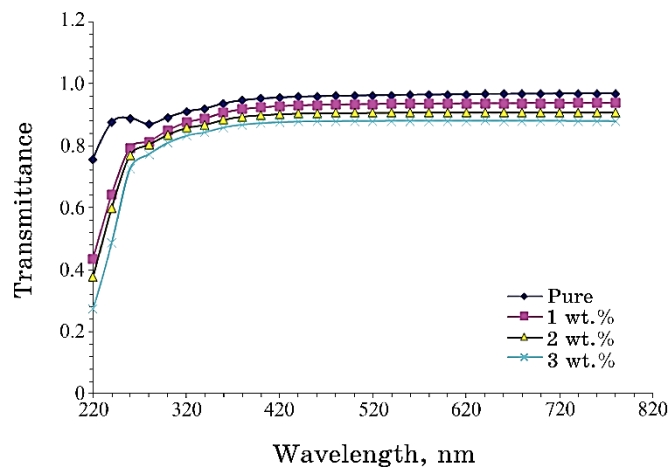


Fig. 3. Change of transmittance with wavelength for PVA/WC nanocomposites.

absorption edge, the incident photon wavelength shortens but its energy remains sufficient to interact with atoms and transmit. Because of photon interactions with the substance, absorbance rises [25, 26].

The relation between transmittance and wavelength for PVA/WC nanocomposites is shown in Fig. 3. We can see, when WC nanoparticles' concentration rises, the transmittance decreases. This procedure results in electron release in their outside orbits, which container absorb electromagnetic energy, because the electron trans-

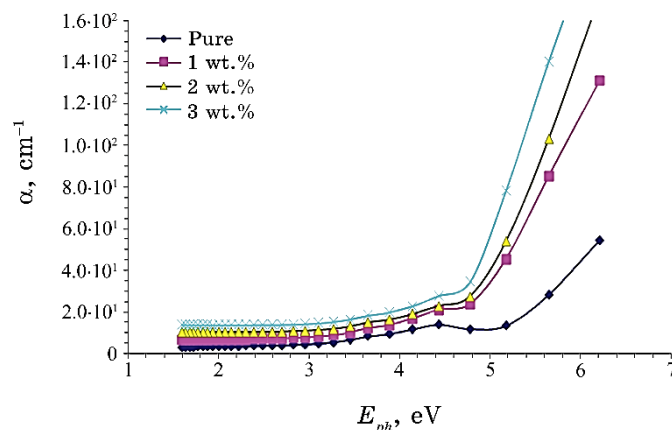


Fig. 4. Absorbance coefficient with photon energy for PVA/WC nanocomposites.

ported to a higher level has occupied vacant locations for energy band. Pure PVA has high transmittance that allows light to pass through PVA, while absorbing some of the incident lights. This is so that the electron connection can be broken, and the electron can be moved to the conduction band (C.B.) [27, 28].

Absorbance coefficient as a function of photon energy of PVA/WC nanocomposites is displayed in Fig. 4. We can see that the absorption coefficient is lowest at high wavelengths and low energies, indicating that there is a little chance for an electron transition, because the energy for the input photon is insufficient to allow the electron to pass the valence band (V.B.) to the C.B. ($h\nu > E_g$) [29]. This shows how the absorption coefficient can influence the type of electron transfer that occurs. Once the absorption coefficient is high ($>10^4 \text{ cm}^{-1}$ in high energies), a direct transition of an electron is anticipated to take place; the energy moments are reserved by the electron–photon interaction. However, since the absorption coefficients are $>10^4 \text{ cm}^{-1}$ at low energies, it is anticipated that an electron will make an indirect transition also that the electronic momentum will be preserved with the help of the adsorption process [30]. The PVA/WC nanocomposites' coefficient of absorbance is fewer than $<10^4 \text{ cm}^{-1}$, demonstrating that the electron transition is indirect in these nanocomposites.

Figure 5 shows difference between photon energy and the absorption edge $(\alpha h\nu)^{1/2}$ for PVA/WC nanocomposites. By connecting the advanced portion of the curve on the x -axis to $(\alpha h\nu)^{1/2} = 0$, we can draw a straight line to visualize the energy gap of this permitted indirect transition. The energy gap values drop with weight percentages of WC nanoparticles rise. The creation of localized levels

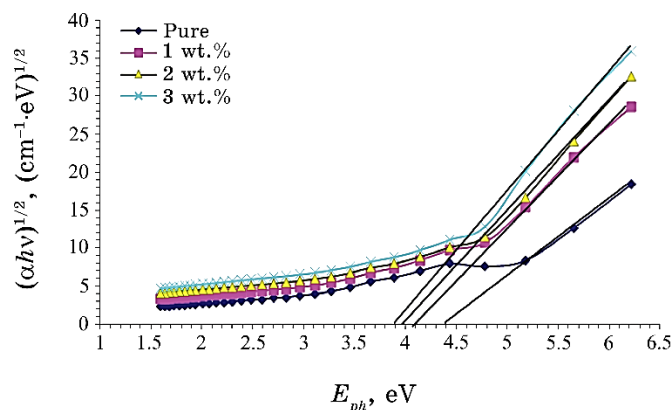


Fig. 5. The relation between absorption edge $(\alpha h\nu)^{1/2}$ and photon energy for PVA/WC nanocomposites.

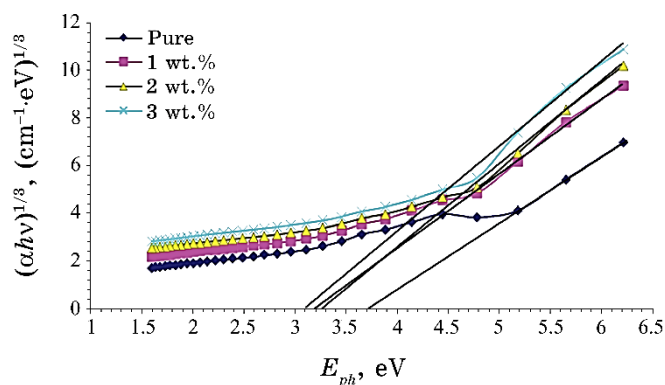


Fig. 6. The relation between $(\alpha h\nu)^{1/3}$ ($\text{cm}^{-1}\cdot\text{eV}^{1/3}$) and photon energy for PVA/WC nanocomposites.

in this prohibited energy gap was credited with causing this. In this instance, as the weight percentage of tungsten carbide nanoparticles rises, the electron ways from V.B. to these limited levels also as a result to this C.B. increase. The density of the localized state rise with concentration of nanocomposites rising because they are heterogeneous rise (*i.e.*, electronic conduction be contingent on the additional concentration) as the weight percentage for tungsten carbide nanoparticles increases [31, 32].

The similar method is used to take into account the forbidden transition for this indirect energy gap, as depicted in Fig. 6.

The relation between refractive index and wavelength for PVA/WC nanocomposites is displayed in Fig. 7. The graph demonstrates that, as density increases, WC nanoparticle concentration to

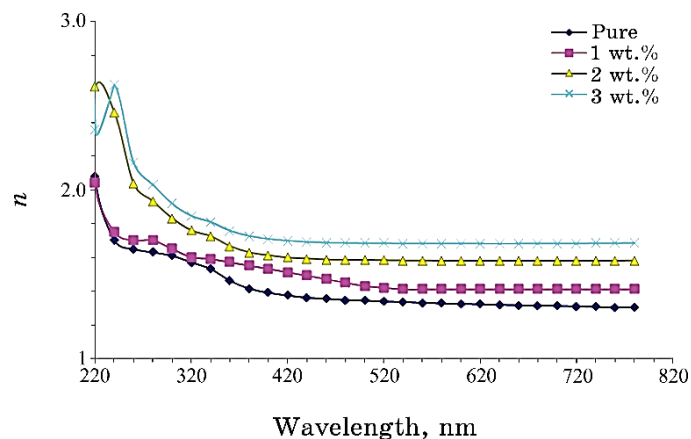


Fig. 7. Refractive index as a function of wavelength for PVA/WC nanocomposites.

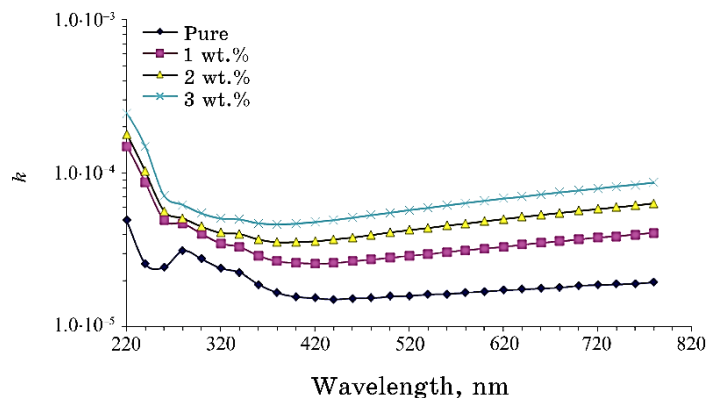


Fig. 8. The relation between extinction coefficient and wavelength for PVA/WC nanocomposites.

PVA, nanocomposites' refractive index increases. Because of its low transmittance, the UV region has high refractive index values, while the visible range has little values because of its high transmittance [33].

The relation between extinction coefficient and wavelength for PVA/WC nanocomposite is shown in Fig. 8. We can note that the extinction coefficient rises as WC nanoparticles' concentration rises. This is attributed to the increased weight percentages of WC nanoparticles and the improved absorption coefficient. This reason suggests that the host polymer structure will change because of the WC nanoparticles [34, 35].

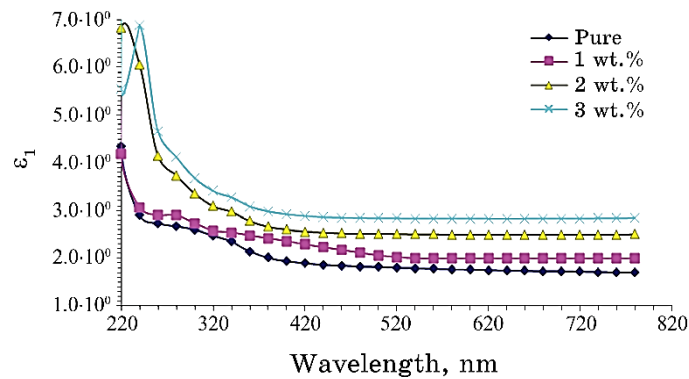


Fig. 9. Variation of real part of dielectric constant with wavelength for PVA/WC nanocomposites.

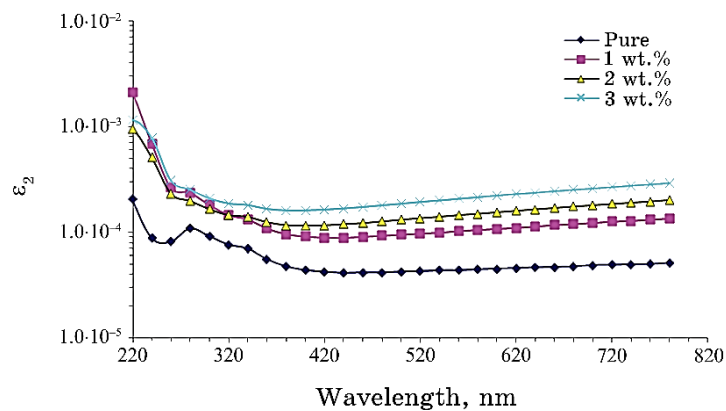


Fig. 10. Imaginary part of the dielectric constant for PVA/WC nanocomposites with wavelength.

The relation between wavelength and real part of dielectric constant for PVA/WC nanocomposites is displayed in Fig. 9. The real part of dielectric constant rises with the rise WC nanoparticles' concentration. Because of the low value of n^2 , this figure demonstrates that ϵ_1 is highly dependent on its k^2 [36, 37].

Figure 10 illustrate the variations of the imaginary part of the dielectric constant with wavelength for PVA/WC nanocomposites. We can see that the ϵ_2 values vary due to the absorption coefficient and dependent on k because of relationship between ϵ_2 with k [38, 39].

Figure 11 shows the change in optical conductivity of PVA/WC nanocomposites with wavelength. As the proportion of WC to the 3 wt.%, the optical conductivity of PVA rises. Because of electrons

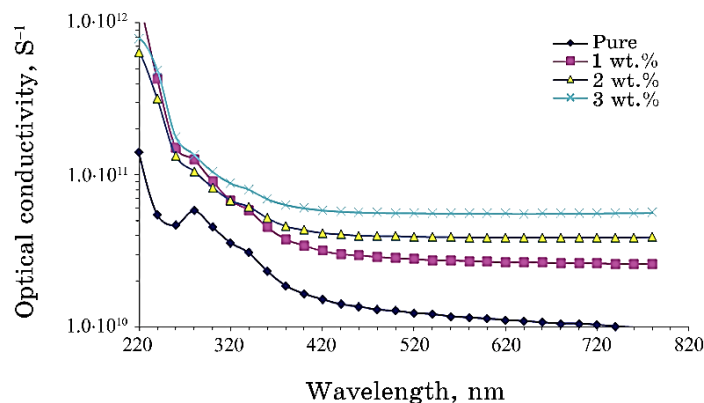


Fig. 11. Optical conductivity of PVA/WC nanocomposites.

can passage the V.B. to the local levels or to the C.B. more easily, thanks to these new levels in this band gap. Therefore, the band gap closes, and conductivity rises [40, 41].

4. CONCLUSION

The results of the optical microscope show that the nanoparticles form a continuous network in films (polyvinyl alcohol), the nanoparticles linked in this network include routes for charge carriers to transport through NCs, causing a shift in the material properties. The absorbance of PVA/WC nanocomposite rises as the concentrations of WC nanoparticles increase, while the transmittance and energy gap drop as the concentration of WC nanoparticles rises. The rise of weight percentages of WC nanoparticles, raise of the absorption coefficient, extinction coefficient, refractive index, real and imaginary parts of dielectric constant, and optical conductivity. Finally, PVA/WC nanocomposites may be considered as promise materials in optoelectronic nanodevices.

REFERENCES

1. B. S. Mudigoudra, S. P. Masti, and R. B. Chou, *Research Journal of Recent Sciences*, **1**: 83 (2012).
2. M. A. Habeeb, *European Journal of Scientific Research*, **57**, No. 3: 478 (2011).
3. M. Ghanipour and D. Dorrastian, *J. Nanomater.*, **2013**: 10 (2013).
4. S. M. Mahdi and M. A. Habeeb, *Digest Journal of Nanomaterials and Biostructures*, **17**, No. 3: 941 (2022);
<https://doi.org/10.15251/DJNB.2022.173.941>

5. M. S. El-Eskandarany and M. Sherif El-Eskandarany, *J. Alloys Compd.*, **391**: 228 (2005).
6. A. H. Hadi and M. A. Habeeb, *Journal of Physics: Conference Series*, **1973**, No. 1: 012063 (2021); doi:10.1088/1742-6596/1973/1/012063
7. Nhiem Tran, Aparna Mir, Dhriti Mallik, Arvind Sinha, Suprabha Nayar, and Thomas J. Webster, *Int. J. Nanomedicine*, **5**: 277 (2010); <https://doi.org/10.2147/IJN.S9220>
8. M. A. Habeeb, *Journal of Engineering and Applied Sciences*, **9**, No. 4: 102 (2014); doi:10.36478/jeasci.2014.102.108
9. X.-H. Gao, C.-B. Wang, and Zh.-M. Guo, Q.-F. Geng, W. Theiss, and G. Liu, *Optical Materials*, **58**: 219 (2016); <https://doi.org/10.1016/j.optmat.2016.05.037>
10. S. M. Mahdi and M. A. Habeeb, *AIMS Materials Science*, **10**, No. 2: 288 (2023); doi:10.3934/mat.2023015
11. M. A. Habeeb and W. K. Kadhim, *Journal of Engineering and Applied Sciences*, **9**, No. 4: 109 (2014); doi:10.36478/jeasci.2014.109.113
12. T. S. Soliman and S. A. Vshivkov, *J. Non-Cryst. Solids*, **519**: 119452 (2019).
13. S. M. Mahdi and M. A. Habeeb, *Physics and Chemistry of Solid State*, **23**, No. 4: 785 (2022); doi:10.15330/pcss.23.4.785-792
14. T. Siddaiah, P. Ojha, N. O. Kumar, and Ch. Ramu, *Mater. Res.*, **21**, No. 5: e20170987 (2018); <https://doi.org/10.1590/1980-5373-mr-2017-0987>
15. M. A. Habeeb and Z. S. Jaber, *East European Journal of Physics*, **4**: 176 (2022); doi:10.26565/2312-4334-2022-4-18
16. A. H. Hadi and Majeed Ali Habeeb, *Journal of Mechanical Engineering Research and Developments*, **44**, No. 3: 265 (2021); <https://jmerd.net/03-2021-265-274>
17. S. Kramadhathi and K. Thyagarajan, *Int. Journal of Engineering Research and Development*, **6**, No. 8: 15 (2013); www.ijerd.com
18. Q. M. Jebur, A. Hashim, and M. A. Habeeb, *Egyptian Journal of Chemistry*, **63**: 719 (2020); <https://dx.doi.org/10.21608/ejchem.2019.14847.1900>
19. A. R. Farhadizadeh and H. Ghomi, *Materials Research Express*, **7**, No. 3: 36502 (2020).
20. A. A. Mohammed and M. A. Habeeb, *Silicon*, **15**: 5163 (2023); <https://doi.org/10.1007/s12633-023-02426-2>
21. M. Chirita, I. Grozescu, L. Taubert, H. Radulescu, and E. Princez, *Chem. Bull.*, **54**, No. 68: 1 (2009).
22. S. M. Mahdi and M. A. Habeeb, *Optical and Quantum Electronics*, **54**, Iss. 12: 854 (2022); <https://doi.org/10.1007/s11082-022-04267-6>
23. N. Hayder, M. A. Habeeb, and A. Hashim, *Egyptian Journal of Chemistry*, **63**: 577 (2020); doi:10.21608/ejchem.2019.14646.1887
24. O. E. Gouda, S. F. Mahmoud, A. A. El-Gendy, and A. S. Haiba, *Indonesian Journal of Electrical Engineering*, **12**, No. 12: 7987 (2014).
25. M. A. Habeeb, A. Hashim, and N. Hayder, *Egyptian Journal of Chemistry*, **63**: 709 (2020); <https://dx.doi.org/10.21608/ejchem.2019.13333.1832>
26. A. Hashim, M. A. Habeeb, and Q. M. Jebur, *Egyptian Journal of Chemistry*, **63**: 735 (2020); <https://dx.doi.org/10.21608/ejchem.2019.14849.1901>
27. S. Choudhary, *J. Mater. Sci., Mater. Electron*, **29**: 10517 (2018).
28. M. A. Habeeb and W. H. Rahdi, *Optical and Quantum Electronics*, **55**, Iss. 4: 334 (2023); <https://doi.org/10.1007/s11082-023-04639-6>

29. M. A. Habeeb and W.S. Mahdi, *International Journal of Emerging Trends in Engineering Research*, **7**, No. 9: 247 (2019); [doi:10.30534/ijeter/2019/06792019](https://doi.org/10.30534/ijeter/2019/06792019)
30. S. Ahmad and S. A. Agnihotry, *Bull. Mater. Sci.*, **30**, No. 1: 31 (2007).
31. M. A. Habeeb and R. S. Abdul Hamza, *Journal of Bionanoscience*, **12**, No. 3: 328 (2018); <https://doi.org/10.1166/jbns.2018.1535>
32. Mojtaba Haghighi-Yazdi and Pearl Lee-Sullivan, *Journal of Applied Polymer Science*, **132**, Iss. 3: 41316 (2015); <https://doi.org/10.1002/app.41316>
33. M. A. Habeeb, A. Hashim, and N. Hayder, *Egyptian Journal of Chemistry*, **63**: 697 (2020); <https://dx.doi.org/10.21608/ejchem.2019.12439.1774>
34. N. K. Al-Sharifi and M. A. Habeeb, *Silicon*, **15**: 4979 (2023); <https://doi.org/10.1007/s12633-023-02418-2>
35. Q. M. Jebur, A. Hashim, and M. A. Habeeb, *Egyptian Journal of Chemistry*, **63**, No. 2: 611 (2020); <https://dx.doi.org/10.21608/ejchem.2019.10197.1669>
36. R. N. Bhagat and V. S. Sangawar, *Int. J. Sci. Res. (IJSR)*, **6**: 361 (2017).
37. M. H. Dwech, M. A. Habeeb, and A. H. Mohammed, *Ukr. J. Phys.*, **67**, No. 10: 757 (2022); <https://doi.org/10.15407/ujpe67.10.757>
38. S. M. Mahdi and M. A. Habeeb, *Polymer Bulletin*, **80**:12741 (2023); <https://doi.org/10.1007/s00289-023-04676-x>
39. R. Dalven and R. Gill, *J. Appl. Phys.*, **38**, No. 2: 753 (1967); [doi:10.1063/1.1709406](https://doi.org/10.1063/1.1709406)
40. M. A. Habeeb and R. S. A. Hamza, *Indonesian Journal of Electrical Engineering and Informatics*, **6**, No. 4: 428 (2018); [doi:10.11591/ijeel.v6i1.511](https://doi.org/10.11591/ijeel.v6i1.511)
41. M. S. Aziz and H. M. El-Mallah, *International Journal of Polymeric Materials*, **54**, No. 12: 1157 (2005).